





An International Journal at the Interface Between Chemistry and Physics

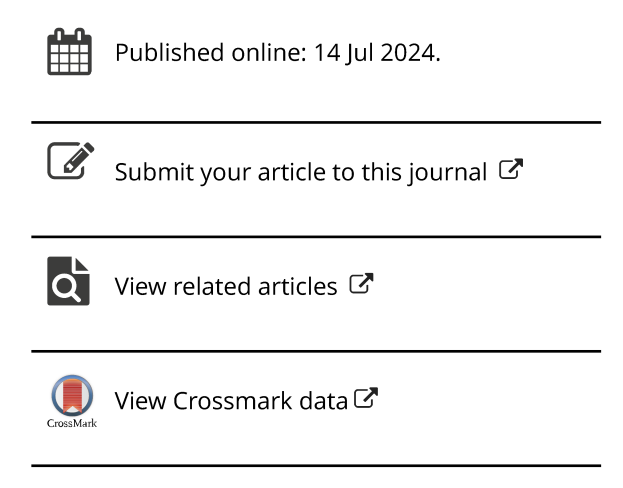
ISSN: (Print) (Online) Journal homepage: www.tandfonline.com/journals/tmph20

The fewest switches surface hopping as an optimisation problem

Alexey V. Akimov

To cite this article: Alexey V. Akimov (14 Jul 2024): The fewest switches surface hopping as an optimisation problem, Molecular Physics, DOI: <u>10.1080/00268976.2024.2376893</u>

To link to this article: https://doi.org/10.1080/00268976.2024.2376893





ALEXANDER NEMUKHIN SPECIAL ISSUE (BY INVITATION ONLY)



The fewest switches surface hopping as an optimisation problem

Alexey V. Akimov (1)

Department of Chemistry, University at Buffalo, The State University of New York, Buffalo, NY, USA

ABSTRACT

Several ways of defining the probabilities of quantum state transitions in nonadiabatic trajectory surface hopping simulations have been proposed and successfully applied to date. Despite their success, there is a question about the uniqueness of the ways to define such probabilities – some formulations require mathematically-motivated but still ad hoc assumptions to resolve the otherwise under-determined problem. In this work, I present a new approach (termed FSSH-3) to define the hop proposal probabilities. Unlike other approaches, it does not require any ad hoc assumptions and is based on the least squares optimisation of certain functionals combined with particular choices of initial conditions for the target variables. A comprehensive comparative study of several established surface hopping methodologies is conducted using several multiple-state model Hamiltonians. The recently reported formulation of the FSSH-2 method is extended to the case of multiple states and validated. It is demonstrated that the performance of all studied methods, including the new FSSH-3 (in two variants) is robust with respect to integration time step used but only if local diabatisation approach is used. Under such conditions, all methods yield nearly identical results, in excellent agreement with fully quantum simulations, even with sufficiently large integration time steps.

$$|i\rangle = \min_{J} \|y - Jx\|_{2}^{2}$$

$$|j\rangle = \min_{J} \|y - Jx\|_{2}^{2}$$

$$P_{i \to j} = \sigma\left(-\frac{\Delta \rho_{ii}}{\rho_{ii}}\right) \frac{\sigma(\tilde{J}_{j,i})}{\sum_{k} \sigma(\tilde{J}_{k,i})}$$

$$P_{i \to i} = \left[1 - \sigma\left(-\frac{\Delta \rho_{ii}}{\rho_{ii}}\right)\right]$$

ARTICLE HISTORY

Received 20 May 2024 Accepted 2 July 2024

KEYWORDS

Trajectory surface hopping; nonadiabatic dynamics; fewest switches surface hopping; global flux surface hopping; FSSH-2

Introduction

The Fewest Switches Surface Hopping (FSSH) algorithm is one of the most popular approaches for modelling quantum-classical nonadiabatic molecular dynamics (NA-MD), with the seminal work of John Tully [1] cited over 4000 times at this point. Although the algorithm is formulated in a very specific way, the definition of the hopping probabilities to different states is based on a rather arbitrary partitioning of the overall hopping probability from a given starting state. Upon a closer look, one can realise that probability partitioning used in the FSSH is only one of the infinitely many possibilities. Thus, although the FSSH algorithm is unique

in its definition, the definitions of the hopping probabilities are not. As a manifestation of this fact, several alternative definitions of hopping probabilities within the framework consistent with that of the FSSH have been proposed in the literature, all addressing various shortcomings of the FSSH-based definitions of hopping probabilities. For instance, Markov state surface hopping (MSSH) defines the hopping probabilities in a naïve way based on quantum populations but enables capturing the superexchange effects [2], global flux surface hopping (GFSH) defines the hopping probabilities based on the analysis of positive and negative population fluxes for all involved states, removes the direct dependence of

the hopping probabilities on the potentially numerically problematic nonadiabatic couplings (NACs) and hence enables using larger electronic integration timesteps in such algorithms [3]. Very recently, a new definition of hopping probabilities within the framework of FSSH was proposed by Araujo, Lasser, and Schmidt [4], dubbed the FSSH-2. Similar to GFSH, the approach is formulated using only the state populations and does not directly involve NACs. However, while the theoretical framework used to define the hopping probabilities in FSSH-2 is solid for 2-state problems, it may be not generalisable to the arbitrary number of states. In summary, although the hopping probabilities of FSSH and FSSH-2 are based on rather intuitive and mathematically-motivated assumptions, they are all formulated in a rather ad hoc way. The logical question one may ask then is: is it possible to define the hopping probabilities between states in a non-ad-hoc, non-human-supervised way and preferably relying only on the state population information at the consecutive timesteps?

In this work, I investigate the possibility of defining and using such a non-ad-hoc, non-human-supervised hopping probability. It is shown that such probabilities can be found by solving a least squares optimisation problem for state-to-state rate constants combined with a physics-motivated partitioning of the state hopping probabilities in proportionality to the found optimal rate constants. The optimisation can be formulated using only the constraints of initial state populations and either the population finite differences or the final state population at the end of each integration time interval. The resulting algorithms are dubbed currentbased or population-based FSSH-3, respectively. The new approach is demonstrated using several N-state crossing models of the Esch-Levine [5] kind. The performance of the FSSH-3 approaches is compared to that of the previously reported FSSH, FSSH-2, and GFSH algorithms. The performance of all algorithms when used with different integration time steps and electronic propagation algorithms is analysed. Finally, the dependence of the FSSH-3 results on the choice of the initial guess of the rate constant matrices is investigated.

Methods

To set the stage for a mathematical formulation of the problem being solved in this work, I first give a general overview of the key elements of the FSSH-like trajectory surface hopping (TSH) algorithms. The distinctions between FSSH, GFSH, and FSSH-2 are discussed next. Finally, I proceed to the formulation of the FSSH-3 approach.

Overview of the generic FSSH-like TSH algorithms

All quantum-classical TSH schemes discussed in this work share a common framework which is summarised in this section. To start with, nuclei are treated as classical particles, that follow the Hamiltonian equations of motion:

$$\dot{\boldsymbol{q}}^{(I)} = \boldsymbol{M}^{-1} \boldsymbol{p}^{(I)}, \tag{1a}$$

$$\dot{\boldsymbol{p}}^{(I)} = \boldsymbol{F}_{a_I}^{(I)}. \tag{1b}$$

The bolded notation is used to denote multidimensional (f degrees of freedom, DOF) vectors, x = $(x_0, x_1, \dots x_{f-1})^T$ or matrices, the dot over the symbols indicates the time-derivatives. The superscript in parenthesis denotes the trajectory index, and the sub-script a_I in Eq. (1b) indicates that the force for the trajectory I is determined according to the active electronic state of that trajectory, a_I . Here, q, p, and F are the nuclear coordinates, momenta, and forces, respectively. The diagonal matrix $M = diag(m_0, m_1, ..., m_{f-1})$ is composed of the masses of each nuclear DOF.

The electronic DOFs are treated quantum mechanically. Namely, the overall electronic wavefunction of the system, $\Psi(r, t; q(t))$ is represented in the basis of electronic adiabatic functions, $\{\psi_i\}$, that depend on electronic coordinates, r, functionally but depend on nuclear coordinates only parametrically, that is $\psi_i = \psi_i(\mathbf{r}; \mathbf{q}(t))$:

$$\Psi(\mathbf{r},t;\mathbf{q}(t)) = \sum_{i=0}^{N-1} c_i(t)\psi_i(\mathbf{r};\mathbf{q}(t)).$$
 (3)

Here, N is the number of electronic basis states, $c_i(t)$ are the time-dependent coherent amplitudes of adiabatic basis functions. The electronic wave function Ψ evolves according to the time-dependent Schrodinger equation (TD-SE):

$$i\hbar\frac{\partial\Psi}{\partial t} = \hat{H}_{el}\Psi. \tag{4}$$

Here, \hbar is the reduced Planck's constant ($\hbar = 1$ in atomic units), $\hat{H}_{el}(\mathbf{r}, t; \mathbf{q})$ is the electronic Hamiltonian operator, such that:

$$\hat{H}_{el}(\mathbf{r},t;\mathbf{q})\psi_i(\mathbf{r};\mathbf{q}(t)) = E_i(\mathbf{q}(t))\psi_i(\mathbf{r};\mathbf{q}(t)). \tag{5}$$

Taking into account Eqs. (3) and (5), Eq. (4) can be simplified to:

$$i\hbar \frac{\partial c_i}{\partial t} = \sum_{j=0}^{N-1} H_{ij}^{vib} c_j, \tag{6}$$

where $H_{ij}^{\nu ib} = E_i \delta_{ij} - i\hbar d_{ij}$ is the vibronic Hamiltonian, $d_{ij} = \langle \psi_i | \frac{\partial}{\partial t} | \psi_j \rangle = \boldsymbol{h}_{ij}^T \boldsymbol{M}^{-1} \boldsymbol{p}$ is the scalar timederivative NAC (also referred to as NAC matrix elements, NACME), and $h_{ii} = \langle \psi_i | \nabla_{\mathbf{q}} | \psi_i \rangle$ is the derivative coupling vector.

The propagated Eq. (6) defines a sequence of timedependent adiabatic amplitudes, $c_i(t)$. This information, perhaps together with the NACME information is used to compute the adiabatic state hopping probabilities, as discussed in the next sub-section. The hopping probabilities are used to stochastically change the index of the active state for each trajectory. Not all proposed hops are accepted. Only the hops $i \rightarrow j$ that can conserve the total energy upon rescaling of nuclear momenta along the derivative coupling vector \mathbf{h}_{ii} can be accepted:

$$\exists \alpha \in \mathcal{R} : \tilde{\boldsymbol{p}} = \boldsymbol{p} - \alpha \boldsymbol{h} : \frac{1}{2} \tilde{\boldsymbol{p}}^T \boldsymbol{M}^{-1} \tilde{\boldsymbol{p}} + E_j$$
$$= \frac{1}{2} \boldsymbol{p}^T \boldsymbol{M}^{-1} \boldsymbol{p} + E_i. \tag{7}$$

If the proposed hop is accepted, the nuclear momenta are adjusted according to Eq. (7), and the active state is reset to the new state onto which the system hopped. If the proposed hop is not accepted because Eq. (7) cannot be satisfied, the proposed hop is rejected (a frustrated hop). In the original prescription of Tully [1], nuclear velocities are reverted upon every frustrated hop. In the present approach, I adapt the Jasper-Truhlar's criterion [6] according to which the momenta along the h_{ii} direction are inverted only if the following two conditions are satisfied: $\mathbf{F}_{i}^{T}\mathbf{h}_{ij} \cdot \mathbf{F}_{i}^{T}\dot{\mathbf{h}}_{ij} < 0$ and $(\mathbf{M}^{-1}\mathbf{p})^{T}\mathbf{h}_{ij} \cdot \mathbf{F}_{i}^{T}\mathbf{h}_{ij} < 0$.

Hop proposal probabilities in FSSH, GFSH, and FSSH-2

Now, that we have revised the overall TSH scheme, we can focus on the key distinguishing element of the FSSH, GFSH, and FSSH-2 algorithms – the formulas to compute the hop proposal probabilities.

FSSH hopping probability formula

The original work of Tully derives the hopping probabilities for a 2-state system and assumes the resulting formula is applicable to systems with any number of states. Although such a solution is possible, it is not unique. To better understand this challenge, it is instructive to resort to the presentation of the FSSH algorithm by Fabiano, Keal and Thiel [7]. One defines the probability of leaving a state *i* during the time interval $[t, t + \Delta t]$ as:

$$\begin{split} P_{i \to *}(t, t + \Delta t) &= \sigma \left(\frac{\rho_{ii}(t) - \rho_{ii}(t + \Delta t)}{\rho_{ii}(t)} \right) \\ &\approx \sigma \left(\frac{-\dot{\rho}_{ii}(t) \Delta t}{\rho_{ii}(t)} \right) \\ &= \sigma \left(-\frac{\Delta \rho_{ii}(t)}{\rho_{ii}(t)} \right) \end{split}$$

$$= \sigma \left(-\frac{\rho_{ii}(t + \Delta t) - \rho_{ii}(t)}{\rho_{ii}(t)} \right). \quad (8)$$

Here, I introduce the σ function (also referred to as sigma function in this work) for the notational convenience:

$$\sigma(x) = xH(x) = \begin{cases} x, & x \ge 0\\ 0, & otherwise \end{cases}, \tag{9}$$

where H(x) is the Heaviside (step) function. The sigma function only ensures that the hopping probability out of a state i is defined only if the population on this state decreases, $\dot{\rho}_{ii}$ < 0. If the population of the state increases, the hopping out of this state would not be consistent with the fewest switches principle. The time-derivative of the population can be replaced with the corresponding expression coming from the TD-SE and involving

$$P_{i\to *}(t, t + \Delta t) \approx \sigma \left(\frac{-\dot{\rho}_{ii}(t)\Delta t}{\rho_{ii}(t)}\right)$$

$$= 2\sigma \left(\frac{\sum_{j=0}^{N-1} Re(\rho_{ij}^* d_{ij})\Delta t}{\rho_{ii}}\right)$$

$$\approx \sum_{j=0}^{N-1} \sigma \left(\frac{2Re(\rho_{ij}^* d_{ij})\Delta t}{\rho_{ii}}\right). \quad (10)$$

It is intuitive and natural to interpret each term in the last sum,

$$P_{i \to j}^{FSSH} = \sigma \left(\frac{2Re(\rho_{ij}^* d_{ij}) \Delta t}{\rho_{ii}} \right), \tag{11}$$

as the hopping probability from state *i* to state *j*. Although this approach is a possibility, it is based on a rather ad hoc assumption. First, strictly speaking, only the total probability of leaving a state is well-defined. The partition of the total probability into channels for hopping into different states is rather arbitrary, based only on the intuitive interpretation of the resulting formula. The partition is not unique as non-unique the representation of any number in terms of a sum of other numbers. For instance, the number 5 can be represented as 1 + 4, 2 + 3, or even 6 + (-1), to show a few of the infinite number of possible ways to partition it. The second approximation, more visible in the current formalism involving the sigma function is that the sigma function of a sum is not the sum of the sigma functions as sneakily introduced in the last step of Eq. (10) to arrive at the FSSH hopping probabilities formula. Note that, the FSSH is commonly formulated using the 'max' function, that is: $P_{i \to j} = max \left(0, \frac{2Re(\rho_{ij}^* d_{ij}) \Delta t}{\rho_{ii}} \right)$, which has the same purpose as the sigma function in the

current notation.

GFSH hopping probability formula

In the GFSH approach, all states are classified into two groups - the states whose population decrease in the integration interval $[t, t + \Delta t]$ (group A, that is: $i \in A$: $\Delta \rho_{ii} < 0$) and the states whose populations increase (group B, that is: $i \in B$: $\Delta \rho_{ii} > 0$). The hopping probability between states belonging to these different groups of states is given by:

$$P_{i \to j}^{GFSH} = \frac{\Delta \rho_{jj}}{\rho_{ii}} \frac{\Delta \rho_{ii}}{\sum_{k \in A} \Delta \rho_{kk}}, i \in A, j \in B.$$
 (12)

Upon a closer look, it can be interpreted as the product of probabilities of leaving the state *i*, $P_{i\rightarrow *} = -\frac{\Delta \rho_{ii}}{\Delta r}$ (the total probability density flux out of state i) and the fraction of the total flux that ends up in a given state j if we start with the state i, $P(j|i) = \frac{\Delta \rho_{jj}}{\sum_{k \in A} (-\Delta \rho_{kk})} =$

 $-\frac{\Delta \rho_{jj}}{\sum_{k \in A} \Delta \rho_{kk}}$, which can be regarded as a conditional prob-

$$P_{i \to i}^{GFSH} = P(j|i)P_{i \to *} \tag{13}$$

As noted above, only the total probability flux out of a given state is rigorously defined in the FSSH, while the splitting of total flux into distinct channels is based on the mathematical structure of the equation. Unlike the FSSH, the GFSH partitions the total flux among different channels based on the corresponding incoming fluxes to the target states, which is a solid physically motivated basis to do so.

FSSH-2 hopping probability formula

The FSSH-2 also starts with the definition of the total outflow probability flux from the starting state i given by the first equality in Eq. (10). $P_{i\to *}(t, t + \Delta t) \approx$ $\sigma\left(\frac{-\dot{\rho}_{ii}(t)\Delta t}{\rho_{ii}(t)}\right) = \sigma\left(-\frac{\Delta\rho_{ii}(t)}{\rho_{ii}(t)}\right)$, where, again, $\Delta\rho_{ii}(t) = \rho_{ii}(t + \Delta t) - \rho_{ii}(t)$. The key distinguishing idea of the FSSH-2 is to use the normalisation condition, $\sum_{i=0}^{N-1} \rho_{ii} = 1$ in the above formula for the total outflow probability:

$$P_{i \to *}(t, t + \Delta t) = \sigma \left(-\frac{\Delta \rho_{ii}(t)}{\rho_{ii}(t)} \right)$$

$$= \sigma \left(-\frac{\rho_{ii}(t + \Delta t) - \rho_{ii}(t)}{\rho_{ii}(t)} \right)$$

$$= \sigma \left(-\frac{(1 - \sum_{j \neq i} \rho_{jj}(t + \Delta t))}{-(1 - \sum_{j \neq i} \rho_{jj}(t))} \right)$$

$$= \sigma \left(\frac{\sum_{j \neq i} (\rho_{jj}(t + \Delta t) - \rho_{jj}(t))}{\rho_{ii}(t)} \right)$$

$$= \sigma \left(\sum_{j \neq i} \frac{\rho_{jj}(t + \Delta t) - \rho_{jj}(t)}{\rho_{ii}(t)} \right) \tag{14}$$

The formula is then interpreted in a spirit similar to the idea of the FSSH, as

$$P_{i \to j}^{FSSH-2} = \frac{\rho_{jj}(t + \Delta t) - \rho_{jj}(t)}{\rho_{ii}(t)}, \tag{15}$$

being the hopping probabilities corresponding to each channel of state transitions. Note that the original work of Araujo and co-workers does not introduce the sigma function, which is reflected in it being omitted in Eq. (15). However, as the authors indicate in their work, Eq. (15) if used directly could lead to incorrect results. As they suggest, when $\rho_{ii}(t + \Delta t) - \rho_{ii}(t) > 0$ and the outflow from the state *i* is zero ($\rho_{ii}(t + \Delta t) - \rho_{ii}(t) = 0$), Eq. (15) would still suggest a $i \rightarrow j$ transition, which should not really occur. Thus, the formula is corrected as:

$$P_{i \to j}^{FSSH-2} = \min \left(-\frac{\rho_{ii}(t + \Delta t) - \rho_{ii}(t)}{\rho_{ii}(t)}, \frac{\rho_{jj}(t + \Delta t) - \rho_{jj}(t)}{\rho_{ii}(t)} \right), \tag{16}$$

This formula taken directly is still potentially problematic if the population of states other than the current active state decreases $(\exists k : \rho_{kk}(t + \Delta t) - \rho_{kk}(t) < 0)$. In this situation, hopping probabilities can become negative. To fix this shortcoming, one simply has to apply the sigma function to each of the two arguments of the minimum function:

$$P_{i \to j}^{FSSH-2} = \min \left(\sigma \left(-\frac{\rho_{ii}(t + \Delta t) - \rho_{ii}(t)}{\rho_{ii}(t)} \right), \\ \sigma \left(\frac{\rho_{jj}(t + \Delta t) - \rho_{jj}(t)}{\rho_{ii}(t)} \right) \right), \forall j \neq i, \quad (17a)$$

$$P_{i \to i}^{FSSH-2} = 1 - \sum_{j \neq i} P_{i \to j}^{FSSH-2}. \quad (17b)$$

It is in this form, the FSSH-2 is now implemented in the Libra software [8,9].

The new approach to hop proposal probabilities via the optimisation problem (FSSH-3)

As demonstrated above for both the FSSH and FSSH-2, the hopping probabilities to certain states are defined mainly by the structure of the equations, by the sumover-states partitioning. Although intuitive, such a way is not physically motivated and is only one of the infinitely many possible other ways. Here, I propose a generic framework that aims to remove this arbitrariness, although in a somewhat 'mathematical black box' way. The hopping probabilities can be defined as a solution to the following optimisation problem. Assume, the vectors of state populations at two times are $\rho(t) = (\rho_{00}(t), \rho_{11}(t), \dots, \rho_{N-1,N-1}(t))^T$ and $\rho(t + \Delta t) = (\rho_{00}(t + \Delta t), \rho_{11}(t + \Delta t), \dots, \rho_{N-1,N-1})$ $(t + \Delta t)^T$. One can then formulate a chemical kinetics problem:

$$\frac{\boldsymbol{\rho}(t+\Delta t) - \boldsymbol{\rho}(t)}{\Delta t} = J(t, t+\Delta t)\boldsymbol{\rho}(t), \quad (18)$$

Here, the matrix element J_{ij} is the rate constant for the $j \rightarrow i$ transition, the positive value indicates that having a population in state *j* initially leads to the increase of the population of state i at the end of the time interval $[t, t + \Delta t]$. Thus, there is a non-zero probability of such a transition. In the spirit of the fewest switches surface hopping principle, one can consider negative values of the I matrix elements as the no-hop criterion. The total probability of hopping out of a state is already well-defined and was introduced above, e.g. Eq. (8). Thus, the probability of staying in the same state is $P_{i\rightarrow i}^{FSSH-3}(t, t+\Delta t) = 1 - P_{i\rightarrow *}$. The probability of the hopping to other states should be proportional to the total probability to leave the initial state as in Eq. (13), $P_{i\to j}^{FSSH-3}(t,t+\Delta t)=P(j|i)P_{i\to *}$ The question is how to determine the conditional probabilities P(j|i). Apparently, such probabilities are proportional to the corresponding rate constants, $P(i|j) \sim \sigma(J_{i,j})$ and should add up to unity, that is $\sum_{i \neq j} P(i|j) = 1$. Note that such a sum

represents the probability of ending up in any of the nonstarting states, provided we have already left the initial state *j*, so the summation skips the index of the starting state, i = j. Alternatively, one can enforce P(j|j) = 0 since the probability of ending in state *j* is zero if we are certain that we have left that state. This condition is also consistent with the definition of the sigma function $\sigma(0) = 0$ and the convention of having $J_{ii} = 0$ in master equation, Eq. (18). It is easy to observe that to satisfy all the above conditions, one can choose:

$$P(i|j) = \frac{\sigma(J_{i,j})}{\sum_{k} \sigma(J_{k,j})}.$$
(19)

To reiterate, the hopping probabilities in FSSH-3 are given by:

$$P_{i \to j}^{FSSH-3} = \sigma \left(-\frac{\Delta \rho_{ii}(t)}{\rho_{ii}(t)} \right) \frac{\sigma(J_{j,i})}{\sum_{k} \sigma(J_{k,i})}, \forall j \neq i, \quad (20a)$$

$$P_{i \to i}^{FSSH-3} = 1 - \sigma \left(-\frac{\Delta \rho_{ii}(t)}{\rho_{ii}(t)} \right). \tag{20b}$$

The next step is to determine the rate constants matrix *J* with the condition of $J_{ii} = 0$, $\forall i$. Eq. (18) can be viewed as a matrix equation:

$$y = Jx, \tag{21}$$

with $y = \frac{\Delta \rho}{\Delta t} = \frac{\rho(t + \Delta t) - \rho(t)}{\Delta t}$ and $x = \rho(t)$. Unlike many other situations when an equation of such kind arises, the unknown here is the matrix J. For a general N-state problem, Eq. (21) imposes N constraints, while there are N^2 unknowns. The problem is underdetermined, meaning that there is no unique solution to it, even for the smallest problem with N = 2. One may try enforcing the unique solution by introducing additional constraints, such as some additional equations relating coherences. However, it is unclear how to introduce such additional equations specifically. For the time being, a plausible practical solution can be given in terms of the least squares fitting, that is via solving the following optimisation problem:

$$J_0 = \min_{I} ||y - Jx||_2^2, \tag{22}$$

Matrix calculus yields a solution that could also be envisioned if one first multiplies both sides of Eq. (21) by x^T from the right and then multiplies both sides of the resulting equation by $(xx^T)^{-1}$ from the right:

$$J_0 = (yx^T)(xx^T)^{-1}. (23)$$

However, this solution is not practical since the matrix xx^T may be non-invertible. Indeed, already for a simple 2-level problem with all population residing on one of the states, that is with x = (1, 0), one runs into trouble, since

$$\mathbf{x}\mathbf{x}^T = \begin{pmatrix} 1 & 0 \\ 0 & 0 \end{pmatrix}$$
, with $\det(\mathbf{x}\mathbf{x}^T) = 0$.

A more practical and robust way to solve the minimisation problem Eq. (22) is to use gradient descent optimisation. Here, it is important to start with a good guess of the J matrix. Specifically, all the rate constants are initialised to be zero initially. The matrix J is then optimised using a steepest descent algorithm until the error $||y - Jx||_2^2$ becomes smaller a specified threshold value ϵ which in this work is set to the value of 10^{-12} . Following the recent nomenclature of Araujo and co-workers, the present approach is dubbed FSSH-3.

Note, that this scheme does not aim to provide significant practical advantages over the original FSSH approach or other TSH schemes. It is intended to demonstrate the conceptual connection between the intuitive approach taken in the FSSH and the optimisation-rooted grounds of the FSSH-3 method. Similar to the GFSH and FSSH-2, the FSSH-3 hopping probabilities do not directly depend on the NACME values, and hence can be used with larger electronic integration timesteps.

Simulation details

In this work, the FSSH, GFSH, FSSH-2 and the new FSSH-3 methods are tested using three linear crossing model Hamiltonians of Esch and Levine [5] (Figure 1). In the diabatic representation, the model Hamiltonians are given by:

$$H_{0,0} = -\omega_0 x, \omega_0 > 0, \tag{24a}$$

$$H_{i,i} = \omega_1 x - i\delta - \epsilon_i, \omega_1 > 0, 0 < i \le N - 1,$$
 (24b)

$$\epsilon_i = \epsilon, \forall i > i_{crit},$$
 (24c)

$$H_{0,i} = H_{i,0} = V, \forall i : 0 < i \le N - 1,$$
 (24d)

$$H_{i,j} = 0$$
, otherwise. (24e)

Specifically, I consider three models: a 2-state Model I, a 3-state Model II, a 5-state Model III, and a 4-state Model IV (Figure 1). For all models, $\omega_0 = 0.015 \frac{Ha}{Rohr}$, $\omega_1 =$

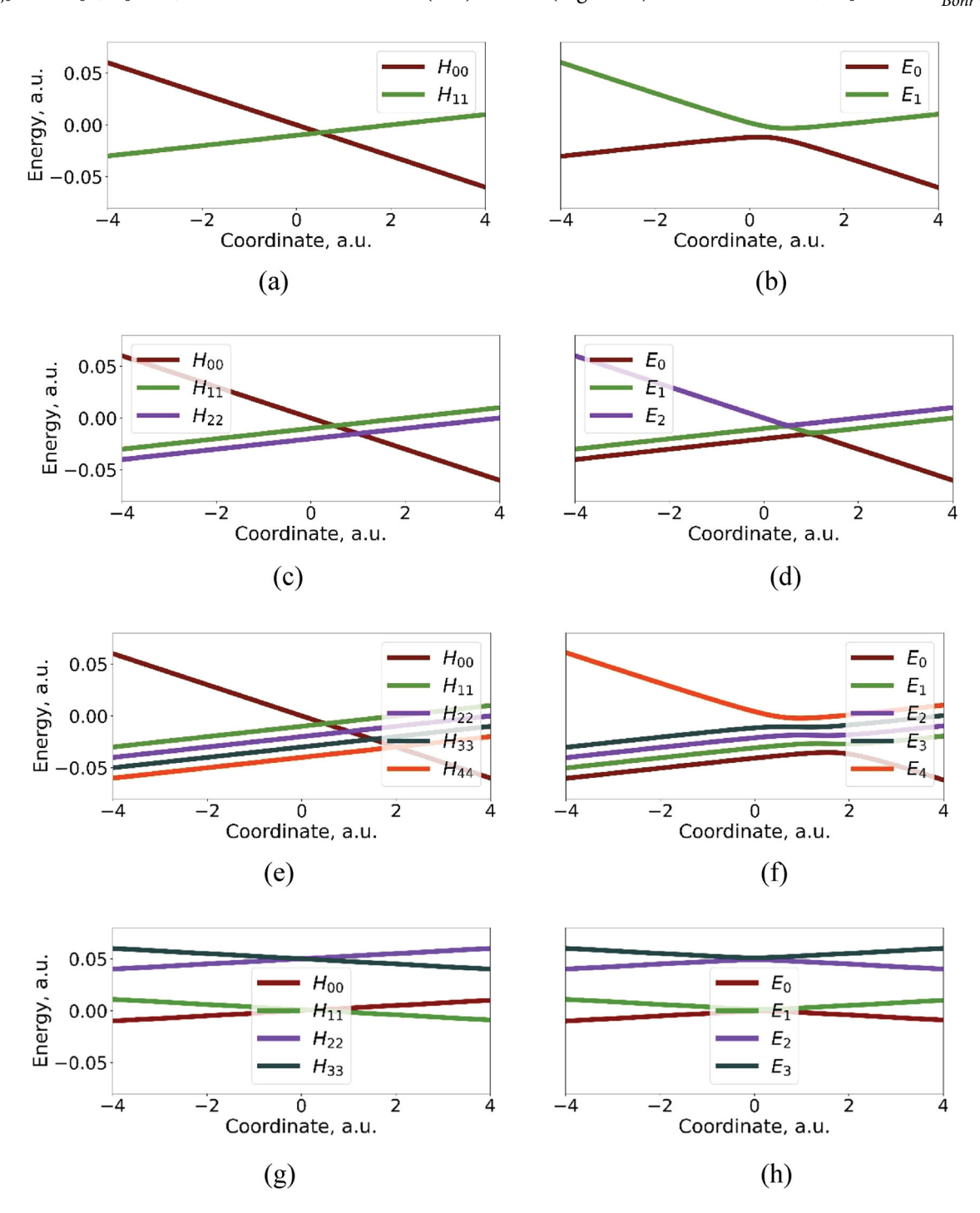


Figure 1. Model Hamiltonians considered in this work: (a, b) Model I; (c, d) Model II; (e, f) Model III; (g, h) Model IV. The left column (a, c, e, g) shows the diabatic energies, right column (b, d, f, h) shows the adiabatic energies.

 $\times \exp\left(-\frac{(p-p_0)^2}{\sigma_p^2}\right).$ (25)

 $0.005 \frac{Ha}{Rohr}$, V = 0.005 Ha, $\epsilon = 0 Ha$, $\delta = 0.01 Ha$. For the first three models, the only difference between them is the number of states and the index of the critical state (Model I: N = 2, i_{crit} = 2; Model II: N = 3, i_{crit} = 3; Model III: N = 5, $i_{crit} = 4$). The last model IV is formulated in a somewhat more general way:

> $H_{ii} = V_{ii} + \omega_{ii}x, \forall i, j \in [0, N-1].$ (25)

The parameters chosen are: $V_{ij} = 0.001Ha, \forall i \neq j, \omega_{ij} =$ $0.0, \forall i \neq j, \quad V_{00} = 0.0, V_{11} = 0.001, V_{22} = V_{33} = 0.05, \\ \omega_{00} = \omega_{22} = -0.0025 \frac{Ha}{Bohr}, \qquad \omega_{11} = \omega_{33} = 0.0025 \frac{Ha}{Bohr}.$ This model is discussed in the work of Araujo et al. [4] in the context of potential limitations of the FSSH-2 approach. It consists of two pairs of crossing diabats, but separated by a sizable gap. The tests are also conducted for two more models of this kind (with N=3 and N = 5 but distinct other parameters), but the results are not discussed in this work since they do not add new conclusions, while the conclusions derived based on the first three models equally hold for the additional models. The details and the results of such calculations are available in the public Zenodo repository [10].

All the TSH methods and model Hamiltonian construction functions are implemented in Libra software [8,9]. The methods reported here are included (or finalised) in the new release of the Libra code, v 5.7.1 [11], prepared together with this work. In all calculations, except when explicitly noted, the initial electronic state is selected as the uppermost adiabatic state (which for this coordinate corresponds to the 0 diabatic state). The mass of the nucleus is taken m = 1800a.u. (where 1a.u. is the mass of the electron, m_e). The average surface hopping populations are computed using 2000 trajectories. The dynamics is integrated for a total time of 1000 a.u., which is sufficient for all the trajectories to pass the crossing region. The TD-SE, Eq. (6), is integrated using the local diabatisation (LD)-based approach [12] similar to that of Granucci and co-workers [13]. The approach automatically accounts for any phase inconsistencies of electronic states that may occur during the dynamics [14] and enables tracking the adiabatic states' identities during the course of adiabatic evolution, a notorious problem encountered in many situations [15]. The total duration of simulations is kept fixed to 1000 a.u. of time, but I consider several integration time-steps varying from $\Delta t = 4a.u.$ to $\Delta t = 40a.u.$ The nuclear and electronic timesteps are chosen to be the same.

The initial nuclear coordinates and moments of the trajectories are sampled from the Gaussian distribution:

$$P(q, p; q_0, p_0, \sigma_q, \sigma_p) \sim \exp\left(-\frac{(q - q_0)^2}{\sigma_q^2}\right)$$

The mean values of the distribution are taken as $q_0 =$ -2a.u. and $p_0 = 10.0a.u.$ in position and momentum directions, respectively. The widths of the distributions correspond to the width of the ground state probability density distribution (Gaussian) of the ground state of a harmonic oscillator with the force constant k = $0.01 Ha/Bohr^2$, that is $\sigma_q = \frac{1}{2\sqrt{mk}}$ and $\sigma_p = \frac{1}{2}\sqrt{mk}$.

Although the present work aims at a comparison of several TSH schemes to the 'reference' FSSH calculations, it is still helpful to compare all the results obtained to the true reference of numerically exact calculations. In this work, the split-operator-Fourier transform (SOFT) integration scheme of Kosloff and Kosloff [16] as implemented in Libra software is used to produce such reference dynamics. The following setups are used in the SOFT simulation. The initial wavefunction is initialised as a Gaussian wavepacket on the adiabatic state corresponding to the initial adiabatic state used in the TSH simulations. The initial coordinate, momentum, and width parameters are chosen to be consistent with the counterparts used to sample the ensembles of trajectories. Note the width parameters used in the wavepacket definition are half of the σ_q and σ_p mentioned above since the latter correspond to the Gaussian describing the probability density rather than the wavefunctions. Similar to TSH simulations, the mass of the particle is chosen to be $m = 1800m_e$. The integration on the grid is conducted for 1000 a.u. of time with the 4.0 a.u. integration timestep. The position grid spacing is chosen to be dx = 0.025Bohr, which is sufficient to accommodate the momenta in the range from - 20 a.u. to 20 a.u. The coordinate extent of the grid is chosen sufficiently large to avoid any wavepacket scattering at the boundaries within the duration of the quantum dynamics simulation.

The input files for conducting all TSH and SOFT calculations reported in this work as well as the visualisation scripts and files are publicly available via GitHub and Zenodo [10]. The repository also contains the results for the additional two models, not discussed in this work. However, the results for these additional models are in line with the discussion presented in the current work using Models I – IV.

Results and discussion

The evolution of the TSH populations of all states in simulations using models I-III are shown in Figures 2-4, respectively. The outcomes are embarrassingly simple to present – all the methods generate nearly identical population dynamics. Furthermore, the results are nearly

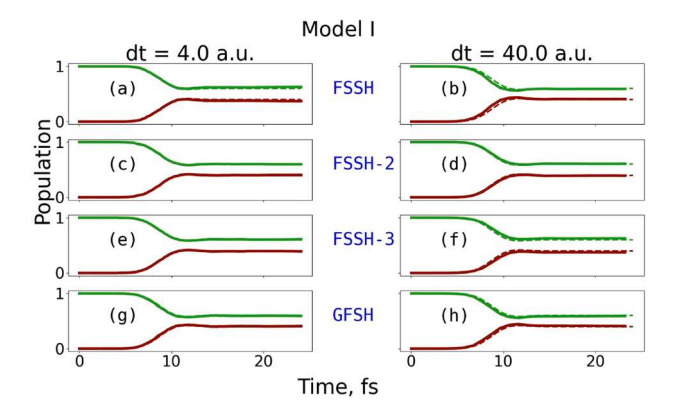


Figure 2. Evolution of the state populations for Model I computed with different methods (rows) and using different integration time-steps (columns). (a, b) FSSH; (c, d) FSSH-2; (e, f) FSSH-3; (g, h) GFSH. The integration time-steps are (a, c, e, g) 4 a.u.; (b, d, f, h) 40 a.u. State colour codes: 1 – green; 0 – red. Dashed lines represent the results of numerically exact calculations. The local diabatisation is used to integrate TD-SE.

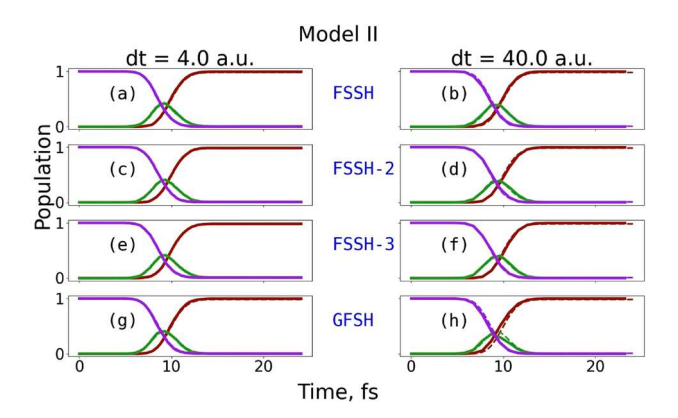


Figure 3. Evolution of the state populations for Model II computed with different methods (rows) and using different integration time-steps (columns). (a, b) FSSH; (c, d) FSSH-2; (e, f) FSSH-3; (g, h) GFSH. The integration time-steps are (a, c, e, g) 4 a.u.; (b, d, f, h) 40 a.u. State colour codes: 2 – purple, 1 – green; 0 – red. Dashed lines represent the results of numerically exact calculations. The local diabatisation is used to integrate TD-SE.

insensitive to the electronic/nuclear integration timesteps used. In principle, this is an expected result given that all four methods are simply different ways of defining the surface hopping probabilities. They do not differ in the level of physics they capture (e.g. none of them introduces decoherence corrections). However, such an ideal agreement of the results yielded by all the methods still carries a notable value. There are at least three main points to highlight.

First, the mere agreement of the FSSH-3 results to those of the well-established FSSH and GFSH methods for multiple models proves that the optimisation-based approach with no ad hoc splitting of the hopping probabilities to distinct states is indeed equivalent to the

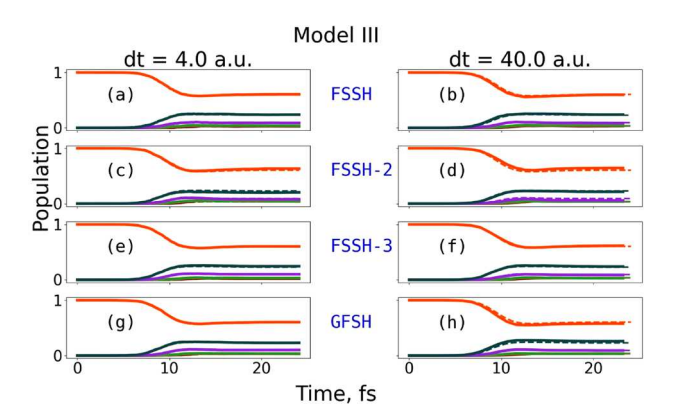


Figure 4. Evolution of the state populations for Model III computed with different methods (rows) and using different integration time-steps (columns). (a, b) FSSH; (c, d) FSSH-2; (e, f) FSSH-3; (g, h) GFSH. The integration time-steps are (a, c, e, g) 4 a.u.; (b, d, f, h) 40 a.u. State colour codes: 4 – orange, 3 – blue-grey, 2 – purple, 1 – green; 0 – red. Dashed lines represent the results of numerically exact calculations. The local diabatisation is used to integrate TD-SE.

pre-determined formulas for the corresponding hopping probabilities, which is the main message of this work.

Second, the current results demonstrate that the FSSH-2 corrected to include the sigma-function transforms does indeed perform as intended, also for the model Hamiltonians with more than 2 states. Note that the original work of Araujo and co-workers discussed the potentially problematic situations for systems with N>2 states and the performance of the method was not clear for model Hamiltonians with more than 2 states. Potentially, for this reason, the reported test included only 2-state problems. The present results demonstrate that the FSSH-2 approach is indeed applicable to systems with more than two states, but the sigma function correction is needed.

Third, the present results are somewhat surprising because the population dynamics practically does not depend on the choice of the electronic/nuclear integration timestep. At the same time, the works reporting the GFSH and FSSH-2 showed a stronger dependence of the results on the integration timesteps, especially for the original FSSH prescription, and demonstrated that the newly introduced methods (GFSH and FSSH-2) produced the converged results with sufficiently large integration timesteps. I attribute this surprisingly robust performance of all methods to the use of the LD approach in the TD-SE integration. To test this hypothesis, the calculations for all three models are repeated using the NAC-based TD-SE integrator, discussed elsewhere [12]. Since the NAC-based integrator does not automatically resolve the electronic wavefunction phase inconsistency problem, a suitable correction is applied [14]. In addition,

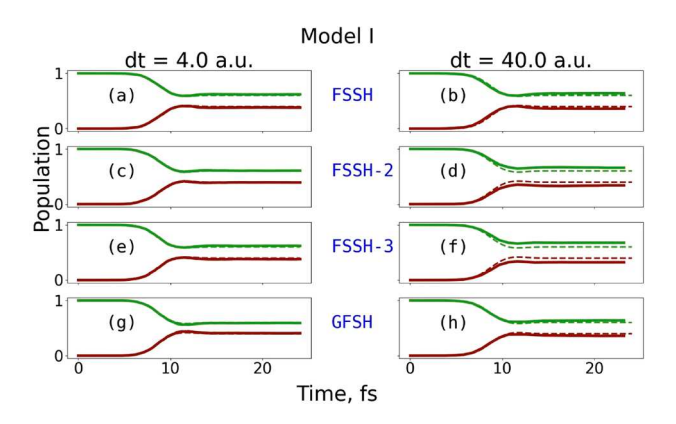


Figure 5. Evolution of the state populations for Model I computed with different methods (rows) and using different integration time-steps (columns). (a, b) FSSH; (c, d) FSSH-2; (e, f) FSSH-3; (g, h) GFSH. The integration time-steps are (a, c, e, g) 4 a.u.; (b, d, f, h) 40 a.u. State colour codes: 1 – green; 0 – red. Dashed lines represent the results of numerically exact calculations. The NAC-based approach together with the phase correction and mincost state tracking are used to evolve coherent amplitudes.

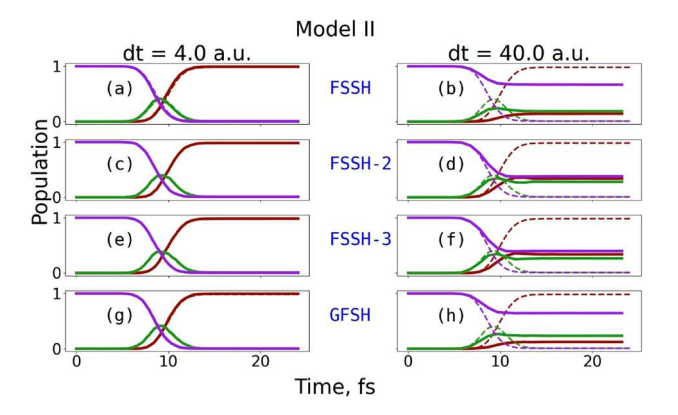


Figure 6. Evolution of the state populations for Model II computed with different methods (rows) and using different integration time-steps (columns). (a, b) FSSH; (c, d) FSSH-2; (e, f) FSSH-3; (g, h) GFSH. The integration time-steps are (a, c, e, g) 4 a.u.; (b, d, f, h) 40 a.u. State colour codes: 2 – purple, 1 – green; 0 – red. Dashed lines represent the results of numerically exact calculations. The NAC-based approach together with the phase correction and mincost state tracking are used to evolve coherent amplitudes.

the state identity is tracked using the min-cost algorithm [15]. The results of such calculations are summarised in Figures 5–7.

Although for sufficiently small integration timestep of 4.0 a.u. the NAC-based integration yields results identical to the LD counterparts and agrees perfectly with the exact reference or LD-based results, one can clearly observe notable deviations of the TSH-based populations from the exact value for larger integration timestep of 40.0 a.u. For the 2-state Model I, the deviations are relatively mild and are larger for the FSSH-2 and FSSH-3 than for the FSSH and GFSH methods (Figure 5). For the 3-state

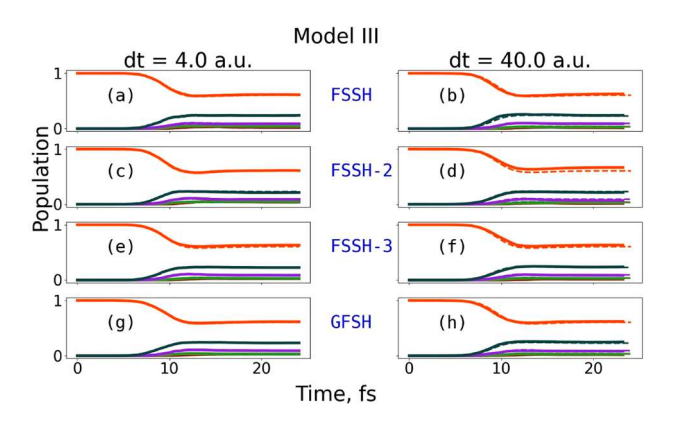


Figure 7. Evolution of the state populations for Model III computed with different methods (rows) and using different integration time-steps (columns). (a, b) FSSH; (c, d) FSSH-2; (e, f) FSSH-3; (g, h) GFSH. The integration time-steps are (a, c, e, g) 4 a.u.; (b, d, f, h) 40 a.u. State colour codes: 4 – orange, 3 – blue-grey, 2 – purple, 1 – green; 0 – red. Dashed lines represent the results of numerically exact calculations. The NAC-based approach together with the phase correction and mincost state tracking are used to evolve coherent amplitudes.

Model II, the deviations are critical. In fact, the population dynamics is completely different from the reference exact dynamics or the corresponding converged TSH calculations (Figure 6). Similar to calculations for Model I, FSSH-2 and FSSH-3 behave similarly to each other, forming one group of methods. The FSSH and GFSH algorithms form another group. Compared to FSSH-2 and FSSH-3, both FSSH and GFSH predict much smaller population decay of the initial state 2 (purple curve). Thus, the former may be considered somewhat superior to the latter since such behaviour is closer to the full depopulation of state 2 observed in the converged calculations and fully quantum calculations. Similar to results of the Model I, the results of Model III show somewhat larger errors for FSSH-2 and FSSH-3 methods compared to those of FSSH and GFSH ones, although still small in absolute values (Figure 7). Although the obtained results suggest the FSSH-2 and FSSH-3 may be somewhat more robust than FSSH and GFSH, it is too premature to make a definite conclusion about it. A more extensive and focused study may be needed, but such a goal goes beyond the scope of the present work.

To summarise, the observed dependence of the computed dynamics on the integration time-step used is much stronger when the NAC-based integration of TD-SE is used instead of the LD. Thus, the goal of fast convergence of TSH calculations with respect to the integration timesteps (what both the GFSH and FSSH-2 methods pursued) is better achieved by using the LD-based integrator instead of the NAC-based one rather than by formulating the hop proposal probabilities in a way that does not explicitly depend on NAC values.

Although the performance of the FSSH-3 approach is quite encouraging, it may be initial guess-dependent. Indeed, since the approach is based on the minimisation of the error defined in Eq. (22), one may end up with one of the multiple possible solutions (local minima), depending on where one starts. The results discussed so far are obtained with the zero initial guess of the rate constants, matrix J=0 in Eq. (22). This is a situation when there are no population fluxes in the system. Starting from such a guess, it is likely that the closest minimum would also correspond to one of the possible combinations of the smallest population fluxes between states.

Such a solution is conceptually close to the idea of the

fewest switches surface hopping. To illustrate the dependence of the FSSH-3 method on the choice of initial guess for the rate constants matrix J, the calculations on all three models are repeated again, but now defining the initial *J* matrix elements as: $J_{i,j} = 1$, if i - j = 1 and $J_{i,j} = -1$ if i - j = -1 and $J_{i,j} = -1$ 0 otherwise (Figures 8-10). One can clearly observe that for Models I and III (Figures 8 and 10) the approach generates population evolutions that are substantially different from the exact results (or the converged TSH ones, which are the same in these models), even though the target error tolerance for the metric $y - Jx_2^2$ is set to 10^{-15} , tighter than the tolerance of 10^{-12} used in the default FSSH-3 calculations. Luckily, the proper state of the rate constants is found for Model II (Figure 9). As before, the calculations are not sensitive to the choice of the integration time-step, since the LD is used to propagate the coherent amplitudes when solving TD-SE.

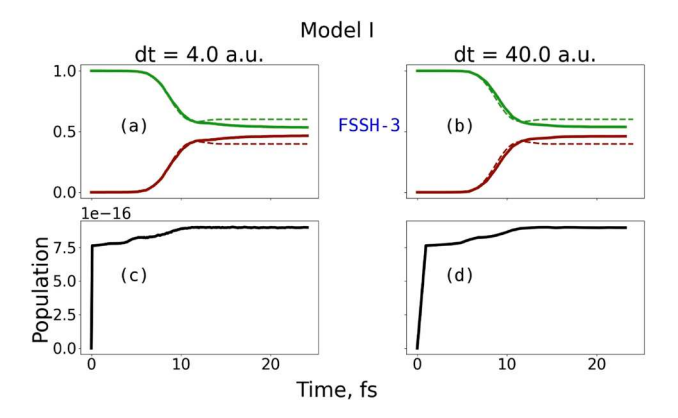


Figure 8. Evolution of state populations for Model I computed with the FSSH-3 method using different integration time-steps (columns), but with the initial rate constants (J matrix) chosen in a specific way described in the text. (a, b) the population dynamics; (c, d) the evolution of the error given by $y - Jx_2^2$. The integration time-steps are (a, c) 4 a.u.; (b, d) 40 a.u. State colour codes in panels (a) and (b): 1 – green; 0 – red. Dashed lines represent the results of numerically exact calculations. The LD-based approach is used to evolve coherent amplitudes.

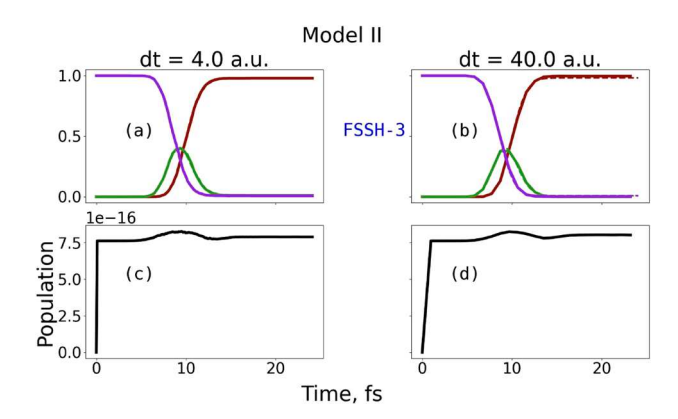


Figure 9. Evolution of state populations for Model II computed with the FSSH-3 method using different integration time-steps (columns), but with the initial rate constants (J matrix) chosen in a specific way described in the text. (a, b) the population dynamics; (c, d) the evolution of the error given by $y - Jx_2^2$. The integration time-steps are (a, c) 4 a.u.; (b, d) 40 a.u. State colour codes in panels (a) and (b): 2 – purple, 1 – green; 0 – red. Dashed lines represent the results of numerically exact calculations. The LD-based approach is used to evolve coherent amplitudes.

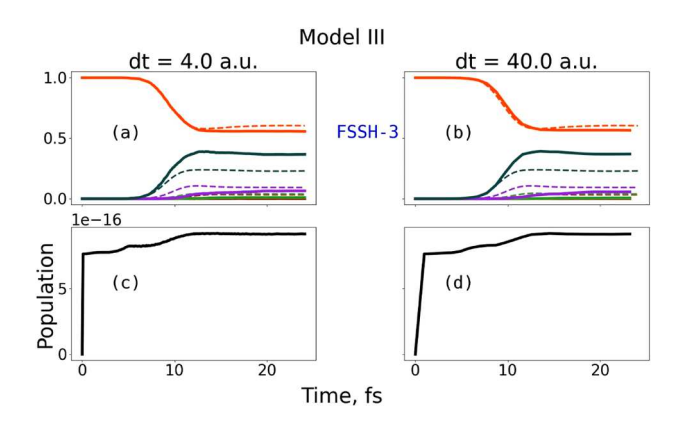


Figure 10. Evolution of state populations for Model III computed with the FSSH-3 method using different integration time-steps (columns), but with the initial rate constants (J matrix) chosen in a specific way described in the text. (a, b) the population dynamics; (c, d) the evolution of the error given by $y-Jx_2^2$. The integration time-steps are (a, c) 4 a.u.; (b, d) 40 a.u. State colour codes in panels (a) and (b): 4 – orange, 3 – blue-grey, 2 – purple, 1 – green; 0 – red. Dashed lines represent the results of numerically exact calculations. The LD-based approach is used to evolve coherent amplitudes.

The found dependence of the dynamics on the initial guess is a purely mathematical problem, which is unlikely related to physical effects such as decoherence or detailed balance. It can be viewed as finding one of the N roots in the N-th order polynomial or N eigenvectors of the rank-N matrix. This work starts with the discussion of the presence of multitude of possibilities for partitioning the total hopping probabilities into pair-of-states-specific contributions. The FSSH-3 solution proposed in this work does not make this problem to fully

disappear. In fact, one of the key results of this work is that one can find a solution that would be the closest to the FSSH by conducting the optimisation with the initial guess closest to the smallest overall currents. The dependence of the dynamics computed by the FSSH-3 on the initial choice of the probability currents means that the FSSH-3 solutions are not unique. However, the hopping probabilities are defined 'automatically' as a result of the optimisation of the identified functionals. In that sense, the approach is free of ambiguity since one needs not define the splitting of the total probability to the pairsof-states contribution in a 'manual' (and sometimes ad hoc) way. The FSSH-3 does not yield a unique solution as this solution depends on the initial guess, but it identifies the solution based on only one human-guided choice - the initial guess of the state of probability currents. This choice is shown to yields the results consistent with other established methods such as FSSH, FSSH-2, and GFSH, thus providing additional support for the hopping probability partitioning given by these methods.

The optimisation of problem for the polynomial with N minima is related to a corresponding root-finding problem for the derivative of such a polynomial, which can also be related to the eigenvalue problem. The present work suggests that there may be several special hop partitioning schemes (stationary regimes), which may be viewed as the eigenvectors of the corresponding problem (e.g. the set of the linear equations derived by setting the derivatives of the error functional with respect to all the fluxes or hopping probabilities to zero, although this is just a loose recipe to arrive to it). The FSSH-3 solution may be one such eigenvectors in the space of the hopping probabilities, likely the one corresponding to the lowest probability flux. In the excited-states terminology, the FSSH (and FSSH-3) could thus be interpreted as the 'ground-state' methodology in the sense that it corresponds to the smallest set of fluxes between the states. Likely, the 'excited-state' approaches are also possible, in which the total probability currents may be not minimal, although it is not clear yet what advantage they would have. In fact, the frequent hopping methodologies similar to those reported by Tully and Preston several decades ago [17], and re-introduced by others more recently [2], may be considered examples of such 'excited-state' methodologies. I stress that in the context of the current paragraph, the terms 'excited-state' or 'ground-state' refer to the level of the methodology itself (the extent to which the total hopping probability currents are 'quantized'), not to the traditional use of such terms to indicate the nature of states between which quantum transitions occur. It may be an interesting topic to explore the 'flux-quantization' surface hopping methodologies in the future, in which non-fewest switches surface hops would be possible. In this regard, the FSSH-3 may serve a convenient starting point.

Finally, I test an alternative formulation of the FSSH-3 approach. It follows the same machinery as described already. The only difference is the definition of the x and y variables in Eq. (21). As a reminder, in the default approach, these variables are chosen as: y = $\frac{\Delta \rho}{\Delta t} = \frac{\rho(t + \Delta t) - \rho(t)}{\Delta t}$ and $\mathbf{x} = \rho(t)$. Together with the initial guess of the choice of the initial \mathbf{J} matrix to be a zero matrix, it makes the FSSH-3 approach. I refer to it as a current-based FSSH-3 formulation. In the modified version, I choose $y = \rho(t + \Delta t)$ and $x = \rho(t)$ and initialise the J matrix to be the identity matrix, J = I. This version is referred to as the population-based FSSH-3. One can recognise that this approach is simply the finitedifference version of the master equation, Eq. (21). Here, the choice of the initial **J** matrix as the identity matrix corresponds to the choice of the zero I matrinx in the current-based FSSH-3 formulation.

As a demonstration, the dynamics computed for all three models using the population-based version of FSSH-3 is shown in Figures 11–13, together with the evolution of the error metric $y - Jx_2^2$ with the convergence threshold set to the default 10^{-12} value. The results of the population-based FSSH-3 calculations perfectly agree with those of the reference (exact) calculations. Thus, such an approach is another valid alternative for the FSSH-3 framework.

In addition to the results obtained for Models I-III, calculations are conducted for Model IV. This kind of model

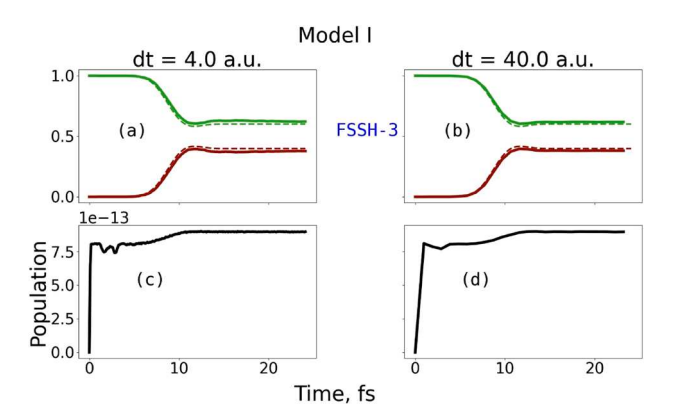


Figure 11. Evolution of state populations for Model I computed with the alternative version of the FSSH-3 (population-based) method using different integration time-steps (columns), but with the initial rate constants (J matrix) chosen in a specific way described in the text. (a, b) the population dynamics; (c, d) the evolution of the error given by $y - Jx_2^2$. The integration time-steps are (a, c) 4 a.u.; (b, d) 40 a.u. State colour codes in panels (a) and (b): 1 – green; 0 – red. Dashed lines represent the results of numerically exact calculations. The LD-based approach is used to evolve coherent amplitudes.

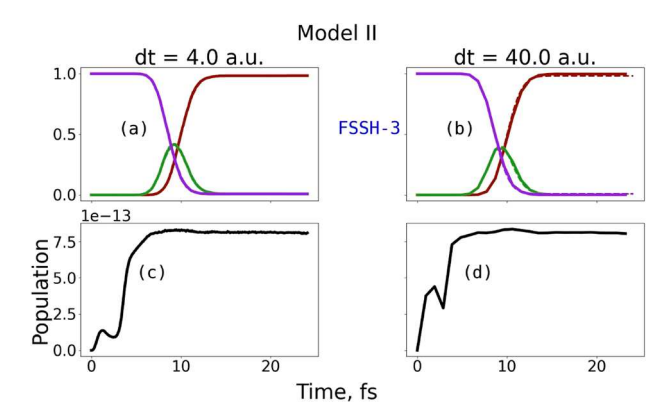


Figure 12. Evolution of state populations for Model II computed with the alternative version of the FSSH-3 (population-based) method using different integration time-steps (columns), but with the initial rate constants (J matrix) chosen in a specific way described in the text. (a, b) the population dynamics; (c, d) the evolution of the error given by $y - Jx_2^2$. The integration time-steps are (a, c) 4 a.u.; (b, d) 40 a.u. State colour codes in panels (a) and (b): 2 - purple, 1 - green; 0 - red. Dashed lines represent the results of numerically exact calculations. The LD-based approach is used to evolve coherent amplitudes.

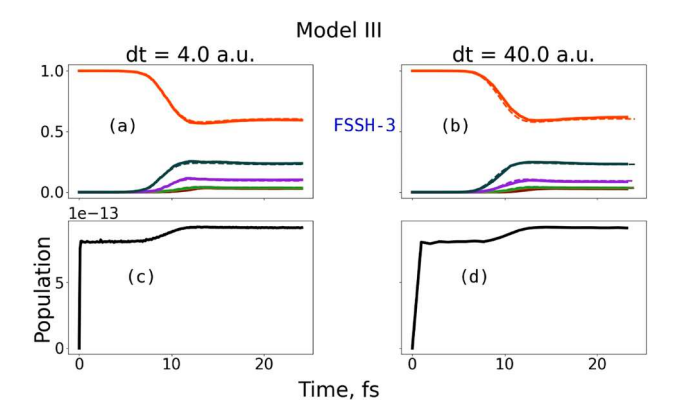


Figure 13. Evolution of state populations for Model III computed with the alternative version of the FSSH-3 (population-based) method using different integration time-steps (columns), but with the initial rate constants (J matrix) chosen in a specific way described in the text. (a, b) the population dynamics; (c, d) the evolution of the error given by $y - Jx_2^2$. The integration time-steps are (a, c) 4 a.u.; (b, d) 40 a.u. State colour codes in panels (a) and (b): 4 – orange, 3 – blue-grey, 2 – purple, 1 – green; 0 – red. Dashed lines represent the results of numerically exact calculations. The LD-based approach is used to evolve coherent amplitudes.

is discussed by Araujo et al. [4] as one of the situations that may be problematic for the FSSH-2 approach due to spurious transitions. Specifically, the separate crossings of state pairs 0-1 and 2-3 mean there may be population transfers $3\rightarrow 2$ and $1\rightarrow 0$. The simultaneous occurrence of such transitions is consistent with the possibility of the population transfer between states separated by a sizable gap and hence weakly coupled, that is $3\rightarrow 0$ or $1\rightarrow 2$. In the situation when the overcoherence effects

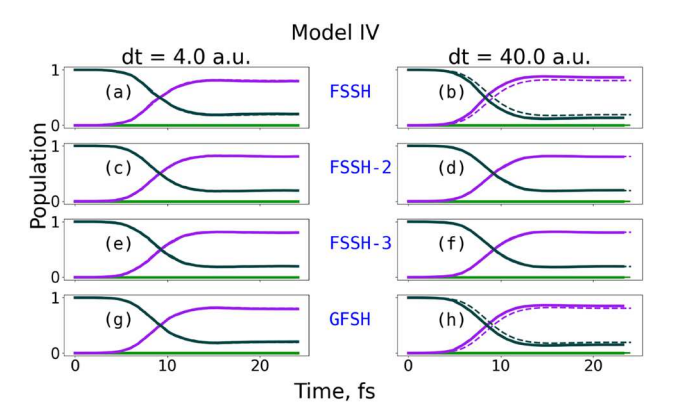


Figure 14. Evolution of the state populations for Model IV computed with different methods (rows) and using different integration time-steps (columns). (a, b) FSSH; (c, d) FSSH-2; (e, f) FSSH-3; (g, h) GFSH. The integration time-steps are (a, c, e, g) 4 a.u.; (b, d, f, h) 40 a.u. State colour codes: 3 – blue-grey, 2 – purple, 1 – green: 0 - red. Dashed lines represent the results of numerically exact calculations. The local diabatisation is used to integrate TD-SE. The initial state in TSH calculations is chosen as the adiabat with index 3.

are not present due to, for instance, decoherence corrections, only one of the pairs of the closely-spaced states should remain preferably populated for the Hamiltonians of type IV. Thus, the initial condition when both states 3 and 1 are populated can be regarded statistically - having 50% of trajectories initiated on the pure state 1 and 50% of trajectories initiated on the pure state 3. The dynamics of each category of trajectories won't be too distinct from what is already discussed above. As a demonstration, Figure 14 illustrates the dynamics in this 4-states model starting on the top adiabatic state. Due to a substantial gap between states 1 and 2, the observed dynamics is effectively the dynamics of a 2-state problem, similar to that of Model I. In this situation, all methods (FSSH, FSSH-2, FSSH-3, and GFSH) yield similar results, also close to the reference exact calculations. One can also observe that FSSH-2 and FSSH-3 both yield a better convergence with respect to integration time step compared to FSSH and GFSH, which start showing deviations from the reference dynamics if the timestep of 40.0 a.u. is used (Figure 14, panels b and h).

However, the dynamics is more interesting when the initial wavefunction is chosen as a coherent superposition of states 1 and 3 (Figure 15). In this situation, one can indeed observe a difference in the dynamics with the hopping probabilities based on NACs (FSSH, Figure 15, panels a and b) from the dynamics with the hopping probabilities defined in the NAC-free way (FSSH-2, FSSH-3, and GFSH). In this case, the FSSH populations behave most closely to the numerically exact simulations, in which the wavefunction is also initialised as a coherent

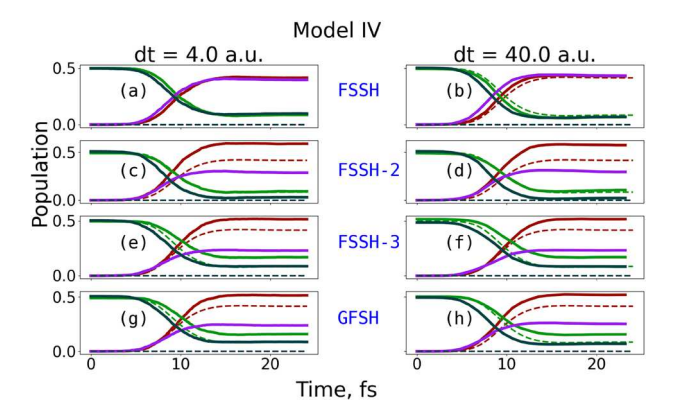


Figure 15. Evolution of the state populations for Model IV computed with different methods (rows) and using different integration time-steps (columns). (a, b) FSSH; (c, d) FSSH-2; (e, f) FSSH-3; (g, h) GFSH. The integration time-steps are (a, c, e, g) 4 a.u.; (b, d, f, h) 40 a.u. State colour codes: 3 – blue-grey, 2 – purple, 1 – green; 0 – red. Dashed lines represent the results of numerically exact calculations. The local diabatisation is used to integrate TD-SE. The initial state in TSH calculations is chosen as incoherent superposition of adiabats with indices 3 and 1 (with equal populations of 0.5 on each). The exact reference (dashed lines) corresponds to the initial coherent superposition on these states.

superposition of two Gaussians placed on states 1 and 3. The population dynamics observed for all NAC-free hopping probabilities are very close to each other. Such calculations do indeed show an increased growth of the population of the lowest state, which can be attributed to spurious hops onto this state, when the quantum population from state 3 decreases intending to transfer to state 2 (according to NACs) and when the quantum population of state 0 increases due to the decay of the quantum population of state 1. Interestingly, the spurious population transfer of this kind observed in FSSH-3 is similar to that of the GFSH, while for both of them it is slightly smaller than for the FSSH-2.

It should be commented though that comparing of the TSH calculations initiated in the coherent state to the analogous numerically exact simulation is a bit tricky. This is because, in the fully quantum dynamics the nuclei experience the Ehrenfest-like forces from the very beginning, while in the TSH simulations, the nuclei for each batch of trajectories only 'know' the corresponding active adiabatic forces, even though the electronic wavefunction can evolve as a quantum superposition of multiple states (of the two initial states in the initial run). Thus, it may be misleading to compare the numerically exact simulations presented to the TSH counterparts when the initial condition is selected as a superposition state. Hence, the seeming 'agreement' of the FSSH population dynamics to that from SOFT simulations is not necessarily the prove that the FSSH results are more physical than the results predicted by other methodologies. In this regard,

the 'spurious' population transfer may still be physical. Unfortunately, it is not possible to set up a completely consistent comparison of the TSH and SOFT simulations to address this question more definitely.

In passing, it is important to keep in mind that although the NAC-free approaches for defining the surface hopping probabilities can be advantageous in a number of way, they are prone to the presence of 'spurious' hops, although as discussed above such 'spurious' hops may still be physical and cannot be ruled out yet. Investigating this conceptual problem could be a next important step in the development of this kind of methodologies. It should be noted that the question of the 'spurious' hops can be avoided when decoherence corrections are incorporated. Indeed, the recent study of Shao et al. [18] demonstrated that different surface hopping schemes such as FSSH and GFSH can yield somewhat different results on their own, but become consistent with each other when decoherence is properly described. This implies that as long as the internal consistency is maintained and proper decoherence is implemented, the question on the appearance of 'spurious' transitions naturally dissolves. In a similar spirit, the recently proposed unified framework of mixed quantum-classical dynamics [19] indicates that different mixed quantum-classical algorithms can yield comparable results if proper decoherence correction is employed.

Conclusions

In this work, I show that the minimisation of the ||y - y|| $|\mathbf{J}\mathbf{x}||_2^2$ functional with respect to the rate-constant matrix *J* is a feasible way to define the hop proposal probabilities for TSH simulations. One can use either the y = $\frac{\rho(t+\Delta t)-\rho(t)}{\Delta t}$ and $x=\rho(t)$ with the initial guess of J=0(current-based FSSH-3) or $y = \rho(t + \Delta t)$ and $x = \rho(t)$ with the initial guess of J = I (population-based FSSH-3). The optimised matrix *J* can be used to construct the hop proposal probabilities in a non-ad hoc way and without explicit dependence on NAC values. It is suggested that the FSSH-3 approach may be regarded a special case of a potentially even more general framework that considers 'quantization' of hopping probability currents (levels of the non-fewest switches surface hopping). Also, the previously reported FSSH-2 methodology is slightly clarified and is shown to work well for problems with more than 2 states.

It is demonstrated that the performance of all methods tested here (FSSH, FSSH-2, FSSH-3, and GFSH) is robust if the local diabatisation approach is used instead of the NAC-based integrators of the TD-SE. Using the LD approach, all methods yield nearly identical results, even if large integration time steps are used. On the

contrary, if the NAC-based integrator of the TD-SE is used, small integration time steps are required to obtain the converged results. If the larger time steps are used, the predicted results are incorrect, but interestingly they show similar results for methods falling within one of the two groups: one - FSSH and GFSH (larger errors) and the other - FSSH-2 and FSSH-3 (somewhat smaller errors). Although the latter observation is not necessarily a general trend, the grouping of the methods in this way is a rather curious phenomenon, although its study is outside the scope of the current work.

It is shown that in simulations for many-level systems where parallel coherent population transfers are possible between several pairs of states, 'spurious' surface hops can emerge for all approaches that use NAC-free hopping probability expressions (FSSH-2, FSSH-3, and GFSH). The FSSH approach does not shows such hops and yields the best agreement with the quantum simulations corresponding to a similar setup. However, due to the intrinsic unavoidable difference in such simulation setups, the final assessment of the physicality of the observed 'spurious' hops remains an open question that may need further investigation.

Disclosure statement

No potential conflict of interest was reported by the author(s).

Funding

This work was supported by the National Science Foundation [Grant OAC-NSF-1931366].

ORCID

Alexey V. Akimov http://orcid.org/0000-0002-7815-3731

References

- [1] J.C. Tully, J. Chem. Phys. 93, 1061 (1990).
- [2] A.V. Akimov, D. Trivedi, L. Wang and O.V. Prezhdo, J. Phys. Soc. Jpn. 84, 0094002 (2015).
- [3] L. Wang, D. Trivedi and O.V. Prezhdo, J. Chem. Theory Comput. 10, 3598 (2014).
- [4] L. Araujo, C. Lasser and B. Schmidt, J. Chem. Theory Comput. 20, 3413 (2024).
- [5] M.P. Esch and B.G. Levine, J. Chem. Phys. 153, 114104
- [6] A.W. Jasper and D.G. Truhlar, Chem. Phys. Lett. 369, 60 (2003).
- [7] E. Fabiano, T.W. Keal and W. Thiel, Chem. Phys. 349, 334 (2008).
- [8] A.V. Akimov, J. Comput. Chem. 37, 1626 (2016).
- [9] M. Shakiba, B. Smith, W. Li, M. Dutra, A. Jain, X. Sun, S. Garashchuk and A. Akimov, Software Impacts. 14 (2022).
- [10] A. Akimov, AkimovLab/Project_FSSH-3: FSSH-3 Data Set, v1.1.0 (Zenodo, 2024).
- [11] A. Akimov, M. Shakiba, B. Smith, M. Dutra, D. Han, K. Sato, S. Temen, W. Li, T. Khvorost, X. Sun, L. Stippell, and A. Jain, Libra v5.7.1 (Zenodo, 2024).
- [12] M. Shakiba and A.V. Akimov, Theor. Chem. Acc. 142, 68 (2023).
- [13] G. Granucci, M. Persico and A. Toniolo, J. Chem. Phys. **114**, 10608 (2001).
- [14] A.V. Akimov, J. Phys. Chem. Lett. 9, 6096 (2018).
- [15] S. Fernandez-Alberti, A.E. Roitberg, T. Nelson and S. Tretiak, J. Chem. Phys. 137, 014512 (2012).
- [16] D. Kosloff and R. Kosloff, J. Comput. Phys. **52**, 35 (1983).
- [17] J.C. Tully and R.K. Preston, J. Chem. Phys. 55, 562 (1971).
- [18] C. Shao, J. Xu and L. Wang, J. Chem. Phys. 154, 234109 (2021).
- [19] G. Li, C. Shao, J. Xu and L. Wang, J. Chem. Phys. 157, 214102 (2022).